REVIEW

Multi-dimensional correlative imaging of subcellular events: combining the strengths of light and electron microscopy

Yingying Su · Marko Nykanen · Kristina A. Jahn ·
Renee Whan · Laurence Cantrill · Lilian L. Soon ·
Kyle R. Ratinac · Filip Braet

Abstract To genuinely understand how complex biological structures function, we must integrate knowledge of their dynamic behavior and of their molecular machinery. The combined use of light or laser microscopy and electron microscopy has become increasingly important to our understanding of the structure and function of cells and tissues at the molecular level. Such a combination of two or more different microscopy techniques, preferably with different spatial- and temporal-resolution limits, is often referred to as 'correlative microscopy'. Correlative imaging allows researchers to gain additional novel structure–function information, and such information provides a greater degree of confidence about the structures of interest because observations from one method can be compared to those from the other method(s). This is the strength of correlative (or 'combined') microscopy, especially when it is combined with combinatorial or non-combinatorial labeling approaches. In this topical review, we provide a brief historical perspective of correlative microscopy and an in-depth overview of correlative sample-preparation and imaging methods presently available, including future perspectives on the trend towards integrative microscopy and microanalysis.

Y. Su · K. A. Jahn · R. Whan · L. L. Soon · K. R. Ratinac ·
F. Braet (✉)
Australian Centre for Microscopy and Microanalysis,
The University of Sydney,
Madsen Building F09,
Sydney, NSW 2006, Australia
e-mail: filip.braet@sydney.edu.au

M. Nykanen · L. Cantrill
Kids Research Institute, Children's Hospital Westmead,
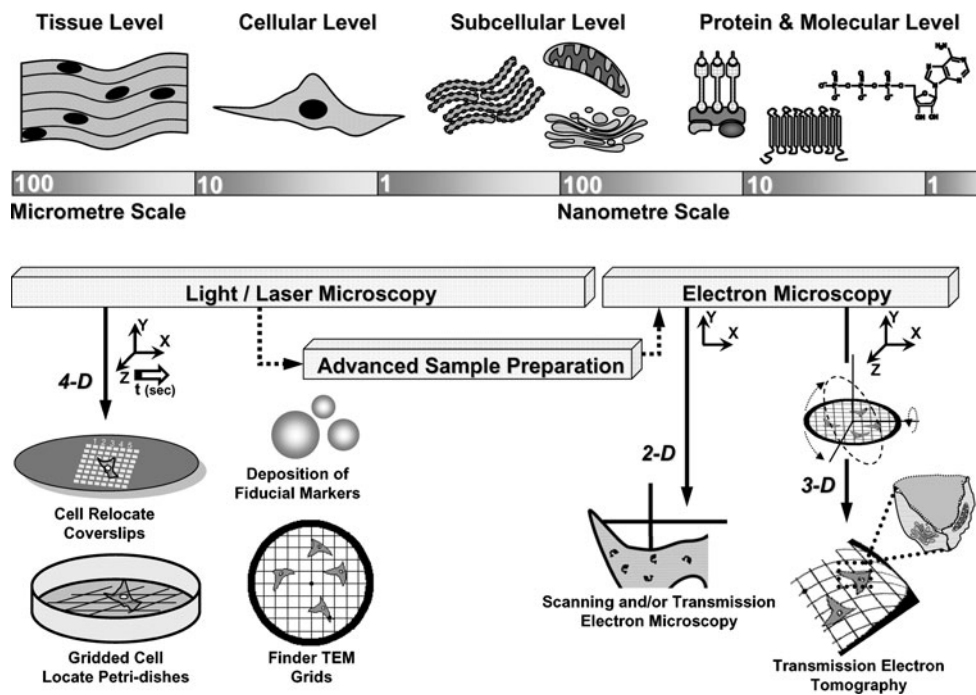Westmead Locked Bag 4001 NSW 2145, Australia

An introduction to cross-correlating microscopy data

Progress in structural biology (Cheutin et al. 2007; Cowieson et al. 2008), advances in optical technologies and software, and developments in electron microscopy (EM) have heralded a new era for combined multi-dimensional biomolecular microscopy. Collectively, these techniques allow imaging and correlation of the fine structure in biological samples, labeled with fluorescent and electron-dense markers, at high spatial and temporal resolutions (Giepmans 2008; Verkade 2008). Indeed, recent studies of cells, tissues, microorganisms, and biomaterials have illustrated the extraordinary possibilities for, and value of, visualizing exactly the same fine structures across different length and time scales and within a relative large sample volume (Nixon et al. 2009; Perinetti et al. 2009; Razi and Tooze 2009). Producing such data demands different microscopes, as well as tools for rapid sample preparation; a typical process includes a live-cell-imaging microscope, rapid-fixation equipment, sample-relocation gear and, finally, a high-end electron microscope (Fig. 1). The application of such a *multimodal cross-correlated imaging approach*, preferably at different resolutions and in conjunction with advanced sample-preparation tools, is known simply as 'correlative microscopy' (CM).

The concept of CM has been around for over 40 years, its tantalizing vision drawing microscopists on a quest for the secret ingredients that could make CM a standard

Fig. 1 Scheme depicting the integration of multidimensional light or laser optical imaging with electron microscopy imaging. This concept is generally defined as 'correlative light and electron microscopy' (CLEM) and aims to bridge the spatial (i.e., length scale) and temporal (i.e., time scale) resolution gaps. CLEM allows the researcher to image and locate specifically labeled targets in living cells, record dynamic processes by light or laser imaging technology (*left*), and finally investigate the same location on the same sample by electron microscopy (*right*). Central to this approach is the use of special sample devices (*bottom left*) that allow the relocation of the structures of interest over different instruments and length scales. Dedicated cover slips, culture dishes, electron microscope supports and fiducial markers are readily available from commercial suppliers for this purpose. Depending on the question to be addressed, the sample can be investigated by scanning electron microscopy (SEM) or transmission electron microscopy (TEM) or both (*bottom right*; see also Fig. 3). It is noteworthy that transmission electron tomography (TET) allows the sample to be analyzed in three dimensions (*3-D*) at high-spatial resolution. *2-D* and *3-D* mean two- and three-dimensional, respectively

microscopy technique. The first paper to coin the phrase 'correlative microscopy' appeared in 1969 (McDonald and Hayes 1969), but it was Geissinger (Geissinger 1974) who, in a brief technical note five years later, elegantly summarized the challenges that must be met when one seeks to capture exactly the same structures on the same microscopic sample by light microscopy (LM) and EM. The first challenge is adapting and fine-tuning the sample preparation to ensure suitability for both imaging modes; the second is guaranteeing that the predetermined area of interest will be examined under both modes; the third, which is intimately linked to the second, is the development of precise and exchangeable sample supports and/or stage facilities that are interchangeable between the different microscope platforms. Today, despite many new technological developments in microscopy, in computer-assisted imaging, and in fluorescent and electron-dense labels, these three challenges still limit the everyday application of CM as a standard approach for all scientists with interests in structural cell biology.

In this topical mini-review, therefore, we will provide a brief overview of a range of modern CM techniques, illustrating how combining imaging platforms can provide new insights on cellular machinery beyond those that can be gleaned from any single microscopy technique. We will then present the latest developments in the field, discussing the move away from correlations between different instruments and towards a fully integrated microscopy approach that uses multiple beam-lines within one instrument.

## Correlative microscopy methods and cross-correlative imaging

The drudgery of early CM methods

Despite the long history of CM as a concept, researchers had to wait until the second half of the 1980s to see the first practical applications of such methods to large sets of samples in order to address specific research questions about biological fine structure (e.g., Albrecht et al. 1989; Donnell et al. 1988; Goodman and Albrecht 1987; Rieder and Bowser 1985; Wynford-Thomas et al. 1986). The CM approaches reported at that time were characterized mainly

by a combination of drudgery, due to the laborious task of finding the same region of sample under different microscopes, and the ingenious application of basic relocation markers, such as microtomy scratches or latex deposits on the sample. Consequently, these pioneering works stand as a tribute to the patience of the practitioners, and to their skills in cross-correlation memory exercises, rather than representing a CM revolution. Nevertheless, those early papers sparked general interest in the CM technique among the scientific community by clearly showing the potential of such approaches to advance cell biology and biomolecular microscopy, provided that easy-to-use methods were to become available. Many researchers quickly began the search for time-saving labeling techniques and simple transfer methods that could facilitate the molecular identification and relocation of exactly the same sample across different microscopes (e.g., Albrecht et al. 1992; Burton et al. 1991; Darien et al. 1995; Deerinck et al. 1994; DeFelipe and Fairén 1993; Hirabayashi and Yamada 1998; Kushida et al. 1993; Miller and Howell 1997; Powell et al. 1998; Robinson and Vandré 1997; Simmons et al. 1990).

Imaging approaches that lead to correlative morphomics

Drawing on this burgeoning activity, researchers have reported different approaches to CM in recent years. These have been successfully applied to a range of different samples, moving from tissues and cells towards the subcellular level (for overview papers, see Biel et al. 2003; Braet and Geerts 2009; Giepmans 2008; Plitzko et al. 2009; Sosinsky et al. 2007; Swanson and Peters 2005), as is evident from a literature search on the topic of 'correlative microscopy' (Fig. 2). With this growing body of literature, it is hardly surprising that different acronyms have cropped up to describe diverse CM approaches. Among the more popular are CLEM (correlative light and electron microscopy), CFEM (correlative fluorescence and electron microscopy), CFSEM (correlative fluorescence and scanning electron microscopy), CFTEM (correlative fluorescence and transmission electron microscopy), CVEM (correlative video-light and electron microscopy), ACLEM (advanced correlative light and electron microscopy), and cryo-CLEM (cryo-correlative light and electron microscopy); these and other acronyms now pepper the fields of cellular microscopy and biomolecular imaging. Despite the variety of appellations, all of these techniques share the common goal of gaining greater depths of ultrastructural information to accumulate morphology–function evidence (i.e., *morphomics*) by applying different microscopes to the same sample (i.e., *correlative morphomics*). In this way, CM provides a higher degree of confidence on the structures of interest, given that information obtained with one method can be
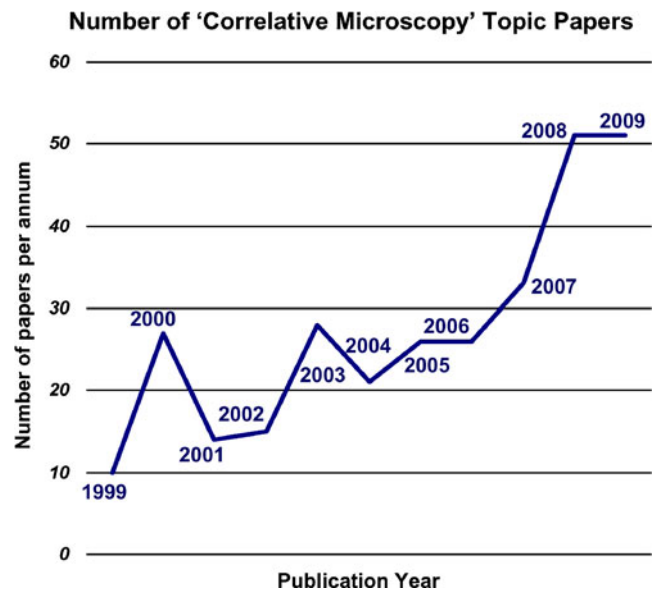

Fig. 2 Literature analysis showing the growth in the number of dedicated 'correlative microscopy (CM)' papers over the past decade. This graph also illustrates the different developmental and application stages of CM. From 1999 to 2002, there was an awareness of the power in cross-correlating microscopy data; however, at that time, there were few hardware and software resources to relocate with precision the same sample across different microscopes. Consequently, CM methods were only used by microscopists with enduring patience. From 2003 to 2006, microscope companies, molecular-probe providers, and laboratory suppliers invested heavily in the development of new technological, chemical, and correlative-imaging tools. This resulted in the widespread application of CM methodology, enabling research on large sets of data. Since 2007, the combination of dedicated hands-on workshops, ease of use of commercial sample-relocation hardware and software, and novel advances in CM approaches has seen the field boom more than ever. The plateau in the numbers of dedicated CM papers in recent times (i.e., 2009) is most likely due, for the most part, to CM technique and imaging developments now being established. In the early days of CM (i.e., prior to the late 1990s), just a handful (approx. 10) of papers were devoted to CM each year. These pioneering papers mainly dealt with the steady development of correlative methods for sample preparation. Source: 'ISI Web of Knowledge—Web of Science'

directly compared to that seen with the other method(s) (Braet and Ratinac 2007).

Classification of CM imaging techniques

Present methods that combine data from LM and EM can be divided into various classes and subclasses, depending on the sample origin and preparation and the visualization approaches employed (Fig. 3). For instance, an obvious classification is based on the EM visualization technique employed: SEM collects primarily topological information, while TEM gathers internal data. The origin of the sample offers an alternative criterion to classify the different CM methods, although this must be closely connected to the visualization technique of choice (Fig. 3). Another classification is based
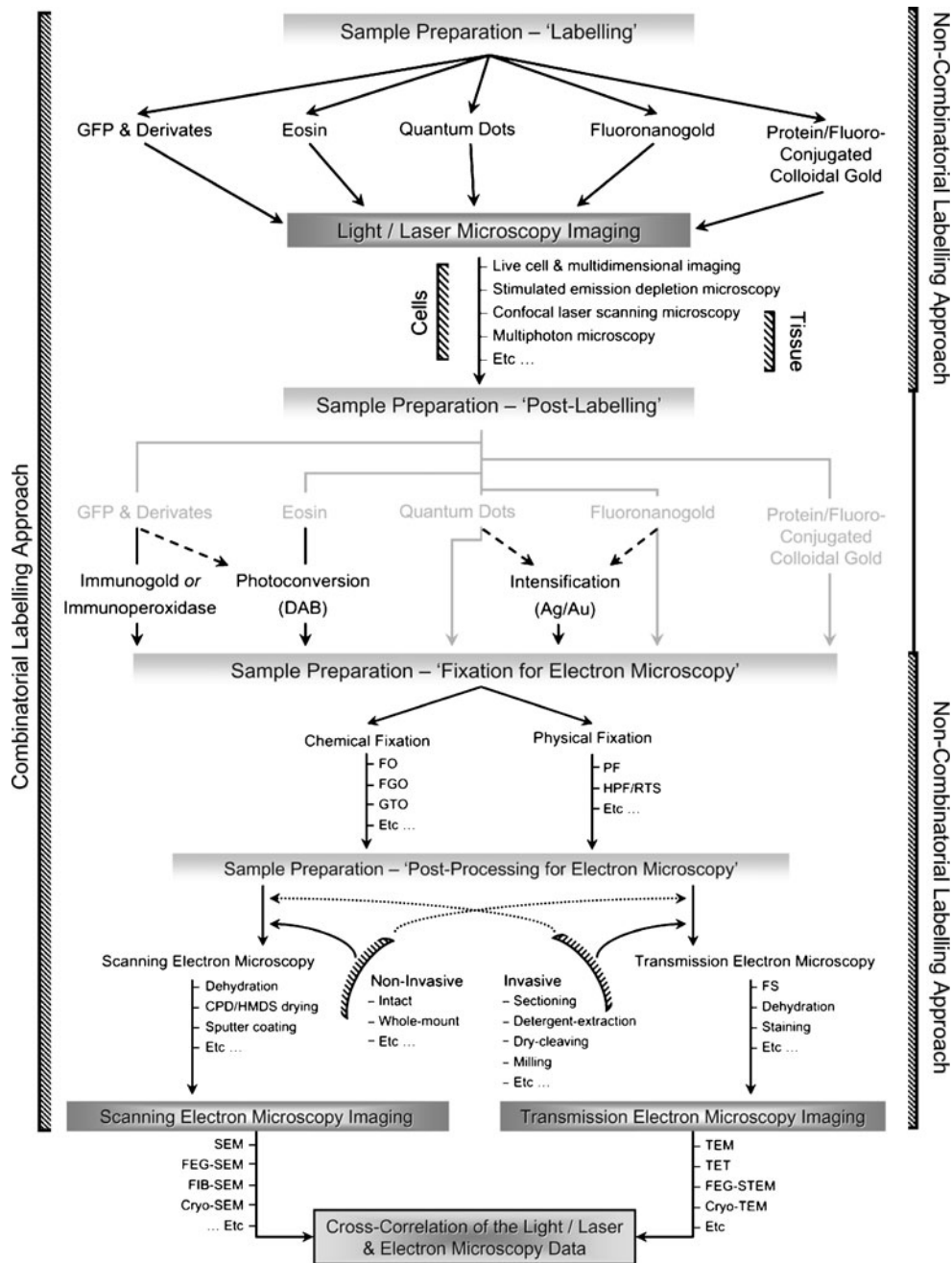
on the choice of sample preparation method(s). Various (non-invasive) sample preparation approaches have successfully enabled CM of intact structures, such as whole-mount cells; however, the majority of approaches deal with (invasive) pre- and post-processing preparation procedures, such as permeabilization, detergent-extraction, sectioning, and the like (Mironov and Beznoussenko 2009). Finally, these various classes can be divided further into subclasses determined mainly by sample fixation (e.g., chemical versus physical fixation) (McDonald 2009; Subramaniam 2005) or labeling (e.g., fluorescent and/or electron-dense tags; see next section) (Giepmans 2008; Sosinsky et al. 2007).

As briefly touched on above, when all intermediate and final sample preparation and labeling steps are completed, the next phase is to image the samples and regions of interest across the chosen microscopy platforms (Fig. 3). Broadly, two major classes of CLEM can be considered. One aims to correlate mainly topological information (e.g., cell-membrane-associated structures) across length scales by combining static or dynamic light/laser data with details of surface morphology obtained by SEM imaging (i.e., CFSEM). The other broad class of CLEM methods is known as CFTEM, and these seek to cross-correlate real-time microscopic subcellular information (e.g., organelles

◀Fig. 3 Schematic depiction of the various approaches and different methods available to perform CM studies. Different sample-labeling and -preparation steps can be considered as well as various imaging approaches, depending on the location of the structure of interest (i.e., whether surface or internal), the planned strategy to detect the (sub) cellular or molecular structure(s) to be identified (i.e., single- vs. double-labeling), and whether those markers are to be visually identified within a single imaging platform (i.e., non-combinatorial labeling) or concurrently across different microscopy platforms (i.e., combinatorial labeling). In the non-combinatorial approach, after labeling and LM examination, samples can be prepared directly for subsequent EM studies. However, some probes, also known as combinatorial probes, permit studies at both the LM and EM scales without the need of any additional post-labeling procedures. It is noteworthy that post-labeling methods involving intensification or enhancement allow the detection of only a single structural feature at the EM level. Next, the sample preparation procedures for EM must also be selected, and these choices largely depend upon whether one wants to cross-correlate light microscopy (LM) data with topological detail (SEM mode) or internal detail (TEM mode) on samples that are chemically fixed or in a 'close to life' state (i.e., physical-fixed). Choices of preparation mode also depend on whether one desires ultrastructural confirmation and concurrent molecular identification of the LM observations at high spatial resolution. Post-processing procedures for SEM studies tend to be less invasive, whereas an inherent limitation of TEM imaging is that the volume of the sample needs to be reduced by sectioning or other related techniques in order to achieve electron transparency. Finally, it is essential to understand, although it is not depicted in this scheme, that in many correlative studies the choice of fixation method and subsequent post-processing starts before the initial 'sample labeling' step for the LM studies. This is especially the case where tissue sections are investigated and where preservation of antigen-reactivity is essential (i.e., physical-fixation approaches will be used). In contrast, cells are easier to deal with as they can be transfected or loaded with (non-)combinatorial probes directly and hence avoid difficulties over antigen preservation. Abbreviations: *Ag/Au* silver/gold enhancement, *CPD* critical point drying, *DAB* 3,3′-diaminobenzidine, *FEG-SEM* field-emission scanning electron microscopy, *FEG-TEM* field-emission transmission electron microscopy, *FIB-SEM* focused-ion-beam scanning electron microscopy, *FO* formaldehyde and osmium tetroxide, *FGO* formaldehyde, glutaraldehyde and osmium tetroxide, *FS* freeze-substitution, *GFP* green fluorescent protein, *GTO* glutaraldehyde, tannic acid and osmium tetroxide, *HMDS* hexamethyldisilazane-drying, *HPF* high-pressure freezing, *PF* plunge freezing, *RTS* rapid transfer system

and proteins) with high-resolution structural information on whole-mounted or sectioned samples by using TEM. In the next section, we present illustrative examples of the application of CFSEM and CFTEM to different samples. We also discuss the most commonly used CM-labeling approaches in-depth as these are essential for identifying fine molecular structures over different imaging platforms, ranging from the microscale to the nanoscale.

Labeling approaches for correlative microscopy

Non-combinatorial versus combinatorial labeling approaches

The strength of CM is the ability to use markers, probes, or labels that can be visualized, directly or indirectly, at the LM level and/or at the EM level (Sosinsky et al. 2007). Combinatorial labeling is the preferred approach in CM as it allows one to trace the tagged subcellular or molecular compartment over the different microscopy platforms with relative ease (see following). We must emphasize, however, that a non-combinatorial approach can be very meaningful as well (Peachey et al. 1996) and often is forgotten by many researchers. Non-combinatorial methods prove especially useful when one seeks to cross-correlate optical data from fluorescently labeled samples with EM data in the absence of electron-dense markers (Fig. 4). This approach also is generally quick, and the samples are less inclined to sample-preparation artifacts because complicated post-labeling and/or other specimen preparation steps are avoided, or at least limited (Braet et al. 2007).

Advanced CM labeling techniques allow enhancement of the site-specific label visualized by LM so that it clearly shows up during subsequent EM imaging. Authentic correlation of dynamic subcellular events and macromolecules in four dimensions (4-D) and with the 'undisturbed' nano-environment in 3-D necessitates optimal specimen preparation (Fig. 3) and also use of suitable combinatorial labeling methods, such as classical fluorophores, fluoronanogold (FNG)-complexes, quantum dot (QD)-conjugated antibodies, or site-specific bio-orthogonal labeling systems. Careful choices must be made, and compromises recognized and accepted, because neither specific labeling procedures nor sample-preparation methods are free of the potential to induce structural artifacts. High-quality CM results should be devoid of sample-preparation and labeling artifacts, and there are no shortcuts to satisfactory accomplishment with any given combinatorial labeling technique. Indeed, whether one uses non-combinatorial or combinatorial CM labeling approaches, the final result depends largely on the compromises made between labeling efficiency and specificity, on the one hand, and the specimen's ultrastructure, on the other. Generally, the most significant trade-off occurs between specificity and size of the label or probe of choice.

Prior to examining in detail the various labeling methods best suited for CM, we should emphasize the two key factors to be taken into consideration when choosing labeling methods. The first is the molecular size of the labels, tracers, or probes to be employed (Fig. 5) as this determines the final spatial resolution that can be achieved at the EM level (Nykänen 2009). The second is the physical nature of the labels/probes: key considerations can include sensitivity to pH or ionic changes, stability over the different beam-lines, life-span during live-cell imaging, binding capacity, and behavior when present in intracellular reductive compartments (e.g., nucleus, cytoplasm, and mitochondria) or under oxidative conditions (e.g., endoplasmic reticulum and cell membrane). Furthermore, inexperienced investigators need to be aware that the labeling procedure and/or tag can also
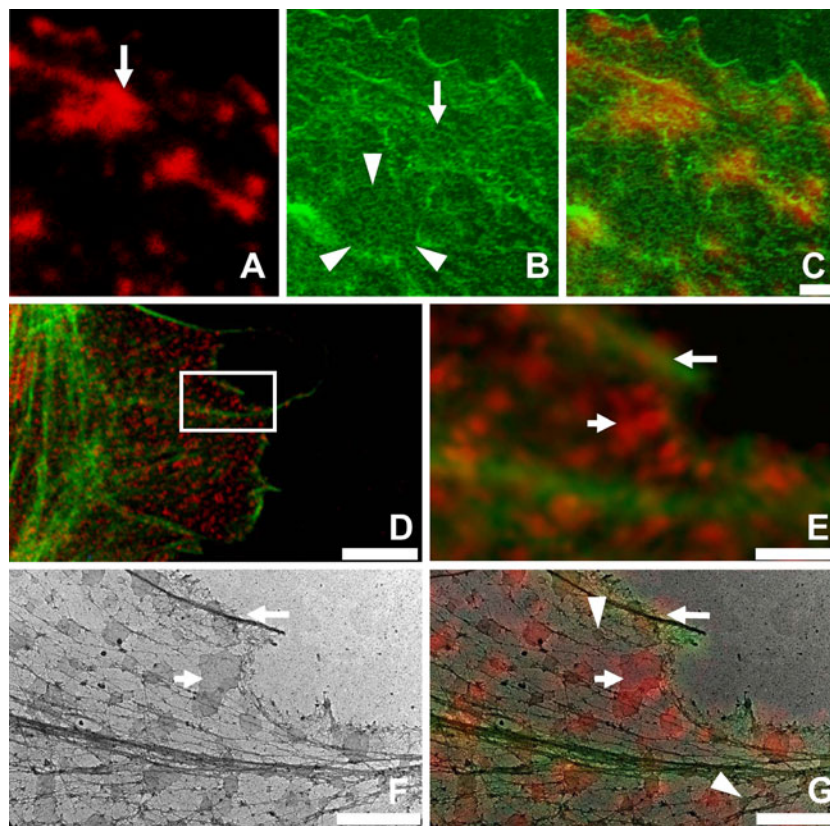
Fig. 4 Examples of the strengths of the 'non-combinatorial CFEM' approach to collect cross-correlative data in the absence of electron-dense markers. **a**–**c** Correlative fluorescence and high-resolution scanning electron microscopy on microfilament-disrupted hepatic endothelial cells in vitro. Filamentous actin staining (**a**) reveals brightly stained cytoplasmatic actin patches (*arrow*), and subsequent topographic investigation of the same cytoplasmic area at the electron microscopic level (**b**) discloses endothelial pores (*arrow*) that make up the sieve plates (*arrowheads*). These pores, also known as fenestrae, typically have a diameter on the order of 200 nm. The merged image (**c**) illustrates that the brightly stained filamentous actin dots coincide with the fine globular topographic elevations present on the thin non-porous cytoplasmic arms and that the sieve plates are devoid of filamentous actin. This observation was crucial in understanding that filamentous actin is involved as a structural scaffold in the support and dynamics of hepatic endothelial pores, illustrating the additional value of applying different imaging techniques to the same cell via straightforward non-combinatorial labeling. For full technical details see Braet et al. (2002, 2007). *Scale bar*: 1 μm. **d**–**g** Correlative fluorescence and transmission electron microscopy micrographs of whole-mounted colorectal cancer cells stained for filamentous actin (*green*) and membrane rafts (*red*). **d** Low-magnification fluorescence micrograph showing the overall actin and membrane raft organization at the cellular level. The *inset box* indicates the area from which images **e**–**g** were taken. *Scale bar*: 10 μm. **e**–**g** High-magnification images show simultaneous localization of the fluorescent-labeled structures (**e**) in combination with the high-resolution TEM information (**f**) and the merged image information (**g**). *Scale bars*: 2 μm. In this example, the authors demonstrated that the smallest membrane rafts could not be detected with the spatial resolution of fluorescence microscopy; however, subsequent TEM investigation allowed easy detection of the small membrane rafts. Note the small membrane rafts devoid of any fluorescent label (*arrowhead*) and the larger membrane rafts which are stained (*small arrow*). *Large arrow* denotes cytoskeleton fibers. For full details, see Jahn and Braet (2008) and Jahn et al. (2009). Reprinted from Jahn and Braet (2008), with permission from Elsevier

adversely interfere with the viability of the sample (Nykänen 2009). From this point onwards, we will examine the commonly used labeling methods available for CM, especially in the context of non-invasive site-specific imaging of living cells and then examine label localization at an ultrastructural level.

Gold particles and colloidal gold complexes

The first papers on CM mainly reported the use of colloidal gold linked to antibodies (Goodman and Albrecht 1987).

Colloidal gold is an excellent electron-dense marker for ultrastructural studies, and the availability of antibodies coupled to gold particles of various sizes—typically in the range between 5 and 20 nm—favor multi-labeling studies of different molecular targets at the same time. However, despite the superiority of this CM technique for labeling different molecular targets at the EM level, the technique is characterized by a low labeling efficiency because of poor penetration rates of the gold-complexed antibodies, which is primarily due to the relatively large size of the gold particles. Permeabilization of the cell membrane by using

Labeling system	size AA	P-L	P-P	ER	MC	P-F	AFL	P-L	P-P	ER	MC	P-F
		INTRACELLULAR						MEMBRANE				
IgG ^	1320		IgG						IgG			
Fab'	880		Fab'						Fab'			
DhaA	296	DHA						DHA				
GFP	238						GFP					
ScFV	220					SFV						
Cutinase	200							CUT				
hAGT	182	AGT						AGT				
DHFR	157	DHR										
FKB12	98							FKB				
Texas R514	38					TXR						
Coiled coil	22							COI				
LplA	17		LAP						LAP			
BirA	15								BIR			
Lanthanide	14									LAN		
Poly-Asp/Zn²⁺	14											ASP
Bungarotoxin	13					BTX						
TC ReAsH*	12			REA						REA		
AcpS PPTase	11							A1S6				
TS RhoBo#	6					RHB						RHB
HisZFit	6								HIZ			
Aldehyde-tag	6							ALH				
NTA-HIS	6								NTA			
Sortag	5							SRT				
Farnesylation	4							FRN				
TGase/Q-tag	4							QTG				

Fig. 5 Schematic representation of the available arsenal of bio-orthogonal CM labeling tags for intracellular and cell-membrane labeling. Most of the labeling complexes can be exploited for live-cell studies and subsequent CM investigation, except for the large immunoglobulins and their fragments exhibited at the *top of the table* (shaded in *blue*). The molecular size of amino acid (*AA*) tags is displayed on the *right column*, and the site-specific labeling method is classified according to the following systems: peptide–ligand (*P-L*), peptide–peptide (*P-P*), peptide–fluorophore (*P-F*), metallic chelation (*M C*), enzymatic reaction (*E R*), or fluorescent proteins (*AFL*) of the target of interest. All labeling options framed by *black squares* can be visualized via an electron-dense marker, such as metals (e.g., Ni²⁺ in Ni-NTA, nanogold, Tb³⁺) or quantum dots (QDs). Labeling systems compatible with DAB-driven photo-oxidation label appear as *dark-blue text*. Most of the marked procedures have been used together with photo-oxidizable conjugates, such as Texas Red and rhodamine and its derivatives, including RhoBo and tetramethyl rhodamine. Labeling systems involving covalent binding are highlighted by *red background* where the bio-orthogonal labeling systems are suitable for long-term in vivo labeling and visualization. The systems containing covalent binding that is not introduced by known photo-oxidation-compatible fluorophores or electron-dense compounds are in *white text*. Labeling systems that exploit metal chelates (e.g., Ni-NTA, Au, lanthanides and QDs) suitable for CM appear in *sky-blue font*. For excellent thematic papers dealing with bio-orthogonal labeling, see Chen and Ting (2005) and Sletten and Bertozzi (2009)

detergents is generally required to increase the gold-labeling efficiency, especially when one wants to stain cytoplasmic components. On the other hand, this technique has shown its merits for the localization of molecular targets associated with, or in close proximity to, the cell membrane. Indeed, combining CM labeling procedures of cell membranes with subsequent freeze-fracture studies of the separated membrane leaflets allows direct visualization of membrane-associated events and proteins (Rash et al.

1998). An example of this approach is given in Fig. 6 in which internalization of Strep-tagged transportan, a peptide capable of translocating across the plasma membrane, was followed by fixation and permeabilization prior to pre-embedding labeling of fluorophore-conjugated antibodies against caveolin and strep-tag. After freeze-fracture replication and LM imaging, the specimen was double-labeled with gold conjugates of 5 and 10 nm (unpublished data, Nykanen et al.). In this example, it was possible to cross-
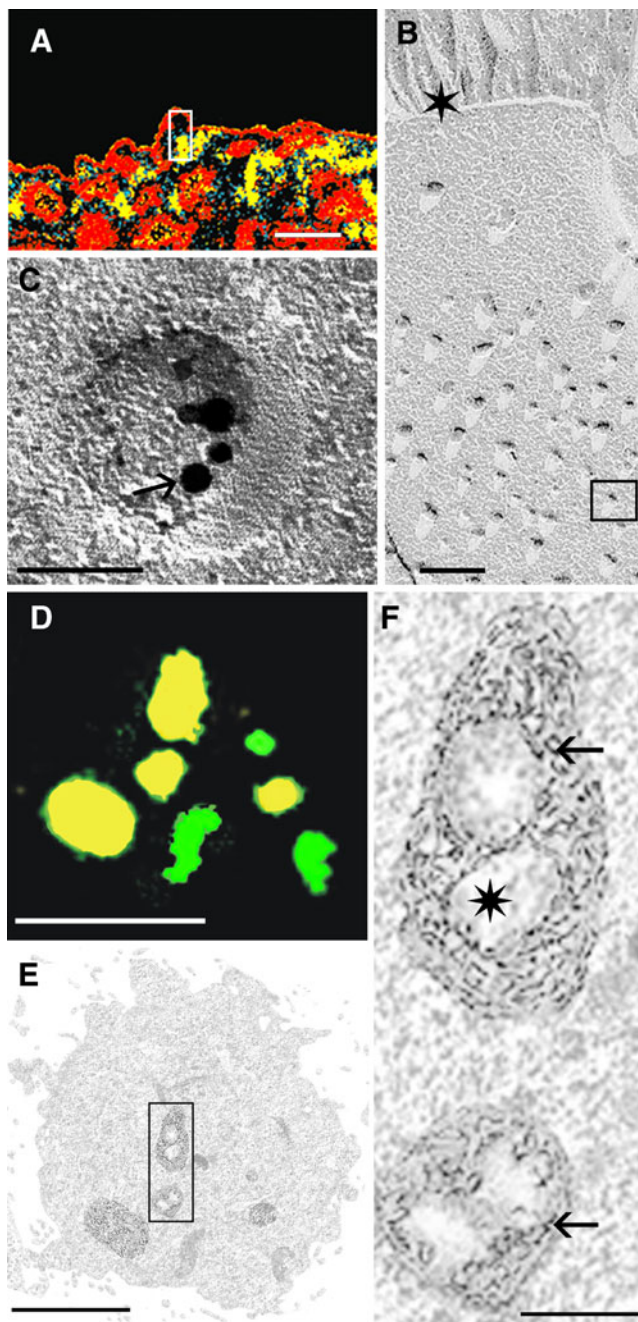
Fig. 6 Two examples of the application of combinatorial CLEM labeling approaches within cultured epithelial cells. **a**–**c** Grid-mapping-assisted CLEM cross-correlation of a Strep-tag-II–fused cell-penetrating peptide, 'transportan', in human lower respiratory epithelium. The epithelial tissue was permeabilized and double-labeled for transportan (mouse anti-Strep-tag conjugated with Alexa 488) and caveolin (rabbit anti-caveolin conjugated with Alexa 568) prior to cryoprotection, freeze-fracture, and platinum–carbon (Pt/C) replication. After replication, the specimen was exposed to sodium dodecyl sulfate, imaged by CLSM, and labeled with secondary antibodies conjugated to gold nanoparticles [mouse anti-immunoglobulin G (IgG) 5-nm gold nanoparticles and rabbit anti-IgG 10-nm gold nanoparticles]. In image **a**, the merged fluorescent information (*yellow*) highlights the co-localization of internalized transportan and caveolin adjacent to the epithelial cell membrane; the *red* signal is positive for concanavalin A (ConA)–Alexa 633 at the cell membrane. *Scale bar*: 3 μm. The EM image (**b**) of the *white box* in **a** is the corresponding fractured region, and this intermediate-magnification image reveals multiple vesicles closely associated with the brush border, which is marked by a *star*. *Scale bar*: 250 nm. Image **c** is a high-resolution TEM image of the region *outlined in black* in image **b**. *Scale bar*: 50 nm. This Pt/C-shadowed replica exhibits well-preserved membranous vesicular structures that are labeled with 5- and 10-nm immunogold antibodies for the molecular targets transportan and caveolin, respectively (*arrow*). **d**–**f** This set of images shows Hela-S3 cells that express the proapoptotic 'recombinant BH3-only protein' with the N-terminal tetracysteine tag ReAsH (*yellow*). The cells have been co-labeled with MitoTracker Green (*green*). After 24 h of live-cell imaging, aldehyde-fixed cells were photo-oxidized with DAB, treated with osmium tetroxide, dehydrated, and then embedded in resin at ambient temperature prior to ultramicrotomy for TEM. Note that the tetracysteine-tagged protein localizes solely in mitochondria (**d**). *Scale bar*: 3.5 μm. The fluorescent signal has been cross-correlated with TEM data, shown in micrograph **e**, over the corresponding cells at the ultrastructural level. *Scale bar*: 2.5 μm. Further investigation of the fine structure in image **f**, which corresponds to the rectangular area marked in **e**, reveals that the mitochondria contain significant intracristal swelling and vacuolization, as shown by the *star*. Small photo-converted DAB precipitates (*arrow*) represent the tagged BH-3-only protein and occur in the proximity of swollen cristae and vacuoles in the mitochondrial matrix. Both of these examples directly illustrate the strengths of the CM approach: light/laser examination of labeled cells allows high-throughput screening, as needed to increase statistical confidence in further analysis; subsequent molecular identification at high spatial resolution then increases our understanding of the intracellular pathways involved in the dynamic processes

correlatively visualize mammalian endocytotic markers and their occurrence in the same epithelial vesicles at the LM and EM levels by using grid-mapping-assisted freeze-fracture replication (Fig. 6a–c). Transportan and caveolin have been co-localized previously in HeLa cells (Säälik et al. 2009), but no CM labeling approach has been exploited so far to unambiguously show their close association.

A significant advance in CM occurred when smaller gold labels (1–3 nm), or so-called FNG particles, were introduced; typical FNG-complexes are approximately 1.4 nm in size (Hainfeld and Furuya 1992). The high surface curvature of these particles makes it less likely that a structured water

dipole layer will build up around the gold surface, and their negative surface charge decreases non-specific binding. Moreover, the FNG enables a much higher labeling density than their colloidal-gold counterparts (Powell et al. 1998). An elegant example of the power of FNG is the 3-D EM study on the internalization of nanogold-complexes by neonatal murine intestinal epithelium (Morphew et al. 2008). While FNG accommodates lower photobleaching of the fluorochrome compared with colloidal gold, PPD and N-propyl gallate can be used as anti-photobleaching agents in combination with FNG labeling (Takizawa and Robinson 2000). Given that nanogold is covalently conjugated to antibodies and does not need supplementary macromolecules

for stabilization, nanogold–Fab' conjugates are the smallest immunogold probes that can penetrate into cells and tissues in a straightforward way. Thus, they can provide the highest possible labeling density and the most nearly quantitative labeling when, for example, gold enhancement has been done. A combination of immuno-nanogold quantification with site-specific molecular labeling (tetracysteine tagging) is particularly useful for the CM approach (see Bio-orthogonal labeling section). Despite its many advantages (Jahn et al. 2007), FNG has seen only limited use in live-cell imaging, an area in which QDs and site-specific bio-orthogonal labeling techniques (see below) have received far more attention.

Photo-oxidation and enzyme-based conversion of 3,3′-diaminobenzidine

Although developed primarily for fluorescent-microscopy applications, low-molecular-weight fluorescent dyes have also played a significant role in labeling for EM studies. Lucifer yellow, for example, is a very stable fluorochrome that is commonly used to study cell function. However, the dye acts as a strong oxidizer under blue light, forming oxygen radicals that oxidize 3,3′-diaminobenzidine (DAB) to form a polymer. This polymeric reticulum is readily stained by osmium tetroxide to produce fine granular, electron-dense precipitates, which can be observed by EM at the sites of the previously imaged fluorescent signals. The DAB polymerization reaction is confined to the labeling site and therefore results in an excellent spatial resolution. A whole range of low-molecular-weight fluorescent dyes has been used in this way, with some of the most interesting applications taking advantage of the unique and specific properties of diffusible dyes. These include CM studies that used, for example, boron dipyrromethene difluoride (BODIPY) ceramide to stain Golgi organelles (Meißlitzer-Ruppitsch et al. 2009) or merocyanidine 540 to display erythrocyte membrane fluidity (Oehring and Halbhuber 1991). The design of ceramide analogs, bearing BODIPY, has produced dyes with higher fluorescent yield, greater photostability, and a concentration-dependent red-shift of the emission spectrum during DAB photo-oxidation. Another high-performance family of dyes is the carbocyanines, which have been used to investigate the structure and dynamics of cell membranes and artificial lipid bilayers. FM 1–43, for example, is an amphipathic molecule that intercalates spontaneously into the outer leaflet of cell membranes without flip-flop or diffusing across the membrane (Fomina et al. 2003). Within this hydrophobic lipid environment, the dye goes through a significant amplification in quantum yield and becomes highly fluorescent, generating up to two-orders of magnitude more signal compared with the yield in aqueous solution.

Successful photoconversion of DAB has also been obtained by using ethidium bromide, tetramethyl rhodamine, Evans fast blue, acridine orange, and nuclear yellow (Lübke 1993). Rhodamine-dextran-amine (Fluoro-Ruby) has been exploited in labeling axons and has been used successfully to photo-oxidize DAB (Schmued and Snavely 1993). In another approach, fluorescent histostains, such as acridine orange, Nile blue sulfate, and safranine T, have been applied during freeze substitution, alongside conventional uranyl-acetate staining, for confocal microscopy and 3-D reconstruction, followed by correlation with EM imaging (Biel et al. 2003). This route provided excellent fluorescent labeling and high-quality preservation for high-resolution EM observation. Finally, correlative studies of cell membranes have been done by photo-oxidizing DAB with the fluorescent ceramide conjugate C6-NBD-Cer, in living and fixed cells (Pagano et al. 1989).

An obvious extension of the DAB photoconversion technique is to apply it to fluorescently labeled antibodies for localization of specific proteins. Deerinck and colleagues (Deerinck et al. 1994) reported that fluorescein and rhodamine do not produce sufficient oxygen radicals to polymerize DAB for detection by EM; however, they simultaneously demonstrated the usefulness of eosin, a brominated derivative of fluorescein, for CM of immuno-localized proteins and in situ hybridization. Although the fluorescence of eosin is only 20% as bright as that of fluorescein, it has nearly a 20-fold higher quantum yield of singlet oxygen. The advantages of this system are that eosin conjugates are smaller than gold conjugates or those of enzyme-based methods and thus have higher rates of penetration into tissues, and the reaction product yields a consistent labeling of the structure of interest and shows minimal diffusion from the reaction site. Eosin-conjugates are commercially available, and the use of eosin–phalloidin, for example, allows the straightforward study of filamentous actin, even for the inexperienced correlative microscopist (Capani et al. 2008). This fluorescent-labeled actin toxin has a great advantage over fluorochrome-tagged anti-actin antibodies, in that phalloidin is a small peptide of only of seven amino acids and thus provides relatively easy penetration into intact or semi-permeabilized cells and tissues.

Enzymatic conversion of DAB by horseradish peroxidase (HRP) represents another approach to CM. HRP-based protein conjugates are one the most frequently used complexes in enzyme-based amplification for immunohistochemical labeling or in diagnostic assays for chemical pathology. This approach can be easily extended to CM by using secondary antibodies or probes complexed to HRP. In the post-labeling preparation, the sample is exposed to hydrogen peroxide, resulting in an electron-dense precipitate on the site of the labeling (Fig. 3). A classical example

of this approach was the study of intracellular transport routes between the Golgi apparatus and the cell membrane (Mironov and Beznoussenko 2009; Mironov et al. 2000). Finally, another labeling approach, based on correlative enzyme-cytochemistry, uses the localization of reaction products of NADH oxidase by cerium-based cytochemistry (Ellis 2008).

Green fluorescent protein

Green fluorescent protein (GFP) and other members of the fluorescent protein (FP) family are photoconvertable domain-tags in CM. FPs can be easily modulated photochemically, and they cover the entire visible spectrum, forming a flexible multiple-labeling toolkit for CFEM studies (Shaner et al. 2005). The majority of FPs are molecular 'highlighters' that can be activated by UV light, which converts them to a protein that emits light at a different peak wavelength than that required for excitation. They can be irreversible (Kaeda, EosFP, and Dendra-2) proteins or reversible (Dronpa, Padron) photo-shiftable proteins. In the correlative approach, FPs permit researchers to tag specific organelles or defined molecular targets and thereby study cell functions within living cells by LM. After appropriate post-labeling treatments to introduce electron-dense markers, EM imaging can be done and readily cross-correlated with the live-cell fluorescence observations (Fig. 3). A major advantage of using FPs or their derivates for CM is that they have high resistance to denaturing during the harsh sample-preparation conditions of chemical fixation. In particular, the antigenicity of FPs generally is retained in chemically fixed preparations, thereby facilitating the subsequent localization of the proteins within the electron microscope by anti-FP antibodies attached to electron-dense markers. Numerous papers have also reported GFP-driven photo-oxidation. Typical examples are GFP fused to a peroxisomal-targeting sequence (Monosov et al. 1996) or to the Golgi enzyme N-acetylgalactosaminyl-transferase-2 (Grabenbauer et al. 2005). However, FPs discharge relatively few singlet-oxygen radicals, which are essential to oxidize DAB, during illumination. This hampers the more widespread use of GFP for CM studies based on photo-oxidation. However, combinatorial labeling approaches for CM that are independent of GFP-driven photo-oxidation have been demonstrated (Mironov et al. 2000). First, the GFP signal is acquired during fluorescent imaging, then anti-GFP antibodies coupled to HRP are used to polymerize DAB for subsequent examination within the EM.

Quantum dots

Quantum dots (QDs) are an attractive labeling approach for CM studies. They are luminescent semiconductor nano-crystals, typically composed of a cadmium-based (CdSe and CdTe) or an indium-based (InP and InAs) crystal core and an outer coating or 'shell'. QDs excel as fluorescent markers, due to their small size and high output, and come with the added advantage that, due to their inorganic crystalline core, they are inherently electron dense. This makes them ideal combinatorial markers for CFEM. QDs have a high signal strength, relatively long fluorescent lifetimes, broad excitation ranges and narrow emission spectra, plus their high brightness means that they can easily allow single-molecule detection (Dahan et al. 2003; Giepmans 2008). The optical properties of QDs are controlled by various parameters, including core size, core composition, shell composition, and surface coating. On confocal laser microscopy systems, blue diode lasers are the best choice for exciting QDs (Deerinck 2008); however, QDs are also ideal for multiphoton excitation (Zipfel et al. 2003), and this causes the least phototoxicity to samples during live-cell-imaging experiments. The emission spectra are mostly influenced by the core size and composition, producing narrow emission maxima that can range from the UV through to the near-IR, and even beyond (Giepmans et al. 2005). Smaller quantum dots (approx. 2 nm) emit at the blue end of the spectrum, while increasing their size (approx. 8 nm) shifts the emission to the red end (Smith et al. 2006). The different diameters of QDs also become useful when their application to EM is considered; double or even triple-immunolabeling is possible because the QDs can be classified according to their different sizes (Giepmans et al. 2005). Developments such as manipulation of QD shapes into rods, tetrapods, and other novel conformations (Peng 2003) could also offer useful tools for differential labeling in EM. Of course, the ability to determine the elemental make-up of the QD core by techniques such as energy-filtered EM might also allow future identification of QDs with different compositions (Nisman et al. 2004).

There are many publications that report the applications and limitations of QDs in fluorescence microscopy (Walling et al. 2009); however, the use of these nanocrystals in CM has been more restricted to date. Nonetheless, there are notable CM studies based on QD labeling, such as the work by Giepmans et al. (2005), Nisman et al. (2004) and Deerinck et al. (2007). Key observations from the development of QD-based correlative labeling techniques have been: (1) the loss of QD fluorescence during osmium-tetroxide fixation, (2) significantly less penetration of QDs into cells or tissues after paraformaldehyde–glutaraldehyde fixation when compared to methanol fixation (Giepmans et al. 2005), and (3) an inability to use multi-labeling techniques if silver enhancement is applied to overcome the relatively low electron density of QDs compared to colloidal gold (Dahan et al. 2003). Correlative approaches that use fixed and embedded

tissues and multiple QD probes have been well established for post-sectioning (Nisman et al. 2004) and for pre-embedding (Deerinck et al. 2007), but the real prize is the correlation of these probes from imaging living systems through to imaging at high resolution. The key to live-cell observation of QD-labeled structures inside cells is obviously an efficient mechanism of QD uptake. Because QDs are not able to permeate cell membranes in the same way as standard organic dyes, various methods have been implemented to introduce them into cells, including injection or microinjection (Dubertret et al. 2002; Larson et al. 2003), the use of transfection agents (Chang et al. 2008), liposome- or electroporation-mediated incorporation (Derfus et al. 2004) or peptide-based and/or aptamer-mediated delivery (Chang et al. 2008; Mattheakis et al. 2004; Zhang et al. 2006). In the final approach, exciting developments in the delivery of large molecules by aptamers and carrier peptide conjugates have been reported (Ho and Leong 2010; Walther et al. 2008). The distance that QDs can penetrate into tissue should also be considered. By using antibody labels to gap-junction proteins, Giepmans et al. showed that QDs were able to penetrate up to 4 μm into fixed cerebellum tissues, whereas immunogold was not able to penetrate this deeply (Giepmans et al. 2005). Clearly, with penetration being the major limitation of QDs by comparison with classical fluorochromes, the future challenge in the use of QDs for CM is going to be to exploit natural and non-perturbing bio-orthogonal pathways for their introduction into living cells and then to take the same cells through rapid high-pressure freezing for EM observation. Concerns about the toxicity of heavy metals, such as cadmium, in the QD cores might be an issue with long-term live-cell experiments as well, but this is leading to innovations such as the development of silicon and diamond-based QDs that might offer a lower potential toxicity in the long term (Fucikova et al. 2009).

Bio-orthogonal labeling

In this final section, we will examine a relative new labeling technique that is gaining more attention in CM because it has few, or even the complete absence of, sample-labeling steps and/or sample-preparation artifacts. Bio-orthogonal labeling aims to uniquely tag site-specific molecular structures in living cells by using chemical reactions that do not interfere with—or, in other words, are 'orthogonal' to—any other molecular constituents in the cells. By employing 'unnatural amino acids' (Reynolds et al. 2008), for example, this method seems to be a very promising avenue to reduce the non-specific off-target labeling inherent in some CM techniques. Bio-orthogonal labeling takes advantage of markers, proteins, or tags with especially low-molecular weights (Fig. 5). As a result, a

high spatial resolution can be achieved compared with early CM methods, such as labeling techniques based on antibodies or high-molecular-fluorescent proteins. In bio-orthogonal CM labeling, the final outcome at the EM level is achieved by attaching photo-oxidizable fluorochromes or electron-dense labels, such as lanthanide metals or QDs, to the unnatural amino acids.

The bio-orthogonal site-specific labeling systems use ectopic expression of a specific gene sequence that encodes for various amino acid tags and the fluorescent protein GFP or its variants (see also, Fig. 5). The amino-acid-associated tags are classified into two major categories: domain tags, which include FPs, and peptide tags, such as epitope-tags, enzymatic tags, and non-enzymatic tags (Lin and Wang 2008). The established site-specific peptide-labeling techniques fall into five main groups: peptide–peptide interaction (P-P), metal chelation (MC), protein–ligand interplay (P-L), enzyme reactions (E-R) and peptide–fluorophore interchange (P-F), as summarized in Fig. 5. The use of a peptide tag directly attached to a fluorophore is one of the most straightforward labeling procedures (e.g., tetraserine-RhoBo, Texas red, single-chain antibodies). Another avenue for tag–probe labeling is to use a mixture of a particular chemical and peptide that cooperatively conjugates a metal ion (e.g., tetracysteine-FlAsH/ReAsH, NTA-His-tag, HisZ-Fit, lanthanide-tag, poly-Asp/Zn^{2+}). An enzymatic reaction that covalently binds a substrate to a given site of a peptide (e.g., farnesylation, TGase/Q-tag, sortag, aldehyde-tag, AcpS PPTase, biotin ligase, LplA) is helpful for long-term cellular visualization. Sunbul et al. have also used an enzyme-catalyzed (phosphophanteinyl transferase) site-specific labeling with coenzyme-A–functionalized QDs to visualize various cell-surface proteins in living cells (Sunbul et al. 2008). Two peptides that form a firm heterodimer can be used as a tag–probe combination ('coiled coil'), while peptide ligands can be employed as a tag that is labeled by a protein probe (e.g., bungarotoxin (BTX), DHFR, hAGT, dehalogenase, cutinase). To overcome the inability of GFP to distinguish intracellular proteins from extracellular proteins, McCann et al. have used combinatorial labeling, based on BTX- or streptavidin-binding motifs, to track the endocytosis of the tagged proteins during pulse-labeling experiments (McCann et al. 2005). This approach was successfully applied to the vesicle-associated protein VAMP2 as a VAMP2-BTX-tag recombinant protein that has been expressed in human embryonic kidney (HEK 293) cells as well as to a receptor tyrosine kinase-BTX-tag [muscle-specific kinase (MuSK)] and BTX-tagged receptors for three neurotransmitters: acetylcholine (nAChRα3), glutamate (mGluR2), and γ-aminobutyric acid (GABA$_A$α3). This clever bio-orthogonal method allowed the team to visualize all exposed proteins on the cell surfaces without noise emerging from intracellular proteins. Simultaneous use of the

streptavidin-binding motif and the BTX-tagging enabled co-localization of the various synaptic proteins listed above.

The success of bio-orthogonal labeling depends critically upon optimizing the expression level of the protein to be tagged by various motifs. In addition to the possibility of inadvertently labeling structures by non-specific hydrophobic interactions, most of the systems can label and cross-react with endogenous components, so that labeling is a competition between the ectopic (exogenous) target protein and these endogenous compounds. Consequently, these techniques will not be successful when off-target labeling occurs, unless the exogenous protein is expressed at much higher levels than the competing endogenous components. For example, the selectivity of tetracysteine (ReAsH) or tetraserine (RhoBo) systems suffers when endogenous thiols or peptides, respectively, interfere with the specific localization of tetracysteine- or tetraserine-tagged proteins. Similar problems can occur in the Texas red–labeled peptide system when the desired fluorescent signal is affected by non-specific staining of mitochondria. This tends to occur because Texas red is charged at physiological pH and hence can accumulate in the mitochondria. Also, endogenous dihydrofolate reductase (DHFR) and O^6-alkylguanine-DNA-alkyltransferase (hAGT) generate background signal. However, by careful choice of the unique characteristics of the expressed protein and its fusion partner (tag), researchers can achieve high specificity of labeling—even at very low protein-expression levels. For example, protein FKBP12, despite its large size (98 amino acids), can be appropriate for localization of target proteins, even when expressed at low quantities, because of its high specificity (Chen and Ting 2005).

Having outlined some of the principles and challenges of bio-orthogonal labeling, we will now provide two examples of the successful use of this approach in CM. The first study used tetracysteine-bisarsenical labeling for localization of ReAsH-tagged filamin in *Drosophila* (Hwang et al. 2009). This kind of labeling, whether by means of FlAsH (fluorescein arsenical hairpin) or ReAsH (resorufin arsenical hairpin), offers several benefits for CM. First, it has an extremely rapid response, with fluorescence emerging within seconds once the biarsenical label is present, in contrast to the minutes or hours needed for GFP to become fluorescent. Second, several cycles of optimization of the amino acid sequence flanking the cysteines have increased the affinity of the biarsenicals for the peptide tags (Martin et al. 2005). Third, this tagging approach covers the entire visible spectrum and is characterized by a strong covalent linkage between the probe and target protein. Fourth, the red label ReAsH can be used for both LM and EM, unlike most other bio-orthogonal labeling systems. Under powerful UV-illumination in fixed specimens, ReAsH produces numerous oxygen radicals that oxidize DAB into an osmiophilic, electron-dense polymer that resides at the precise location of

the exposed ReAsH. Importantly, the ReAsH-driven polymerization of DAB is less dispersed than the photo-oxidized precipitate resulting from GFP or other photo-oxidation systems.

In the second example, Nykänen and colleagues have recently employed ReAsH for fluorescent imaging and then used ReAsH-driven photo-oxidation for subsequent CM studies (unpublished data). In this study, the trafficking of 'BH3-only pro-apoptotic protein' (168 amino acids) was followed in mammalian cells (Fig. 6d–f). The application of this labeling technique was central to answering the question of whether the fine structural and molecular changes observed at the sub-mitochondrial level were introduced by sample preparation or represented a genuine morphological change due to protein trafficking. The appearance of these intra-mitochondrial vacuoles by etoposide-induced apoptosis in HeLa cells had been described earlier (Frey and Sun 2008; Sun et al. 2007). However, it had been postulated that chemical fixation and EM sample-preparation at ambient temperature was responsible for such intra-mitochondrial ultrastructure. In Nykänen's study, over-expression of the protein together with in vitro induction of cellular apoptosis has facilitated successful trafficking of the BH3-only pro-apoptotic protein into mitochondria. When combined with specimen preparation by high-pressure freezing and freeze substitution, the ReAsH-driven photo-oxidation of DAB revealed the swelling of mitochondrial matrix (due to loss of the mitochondrial membrane potential) and ultrastructural changes in the inner membrane associated with emergence of large vacuoles.

To round out this section, we must place the success of tetracysteine-tagging, as outlined in the foregoing examples, in the context of the known limitations of these labels. The first issue, as already mentioned above, is off-target labeling. Given that the biarsenical compounds maintain considerable affinity for monothiols, off-target labeling limits the sensitivity of this method to an order of magnitude less than that of GFP. One way around this problem could be the use of 2-mercaptoethanol acid, which has been reported to double the number of collected photons from ReAsH molecules (Park et al. 2004). Another proposed solution has been exposure of the labeled cells to more stringent staining conditions where binding of fluorescent tracer to native tetracysteine motifs—i.e., off-target labeling—is reduced. In many cases, however, the more stringent staining circumstances have not completely eradicated non-specific binding. The second major concern is potential toxicity when living samples are under investigation. Besides aggressive hydrogen peroxide produced by excitation of the fluorophores, the presence of arsenic might be a concern, although acute toxicity can be avoided by the use of dithiol antidotes as was done in the study by Hwang et al. (2009).

Conclusions and future outlooks

There is no better way to conclude this review than by quoting Ben Giepmans in one of his recent papers: "Exaggeratedly stated, with fluorescence microscopy, you almost see nothing, i.e., only your fluorescent signal(s); with EM, you see everything, i.e., organelles, macromolecules and membranes" (Giepmans 2008). Of course, die-hard fluorescence and laser microscopists will dispute this, appealing to the rapidly growing arsenal of advanced-imaging and data-analysis techniques, such as multiphoton microscopy, photo-activated localization microscopy (PALM) and, recently, stimulated emission depletion microscopy (STED). However, no one will dispute that CLEM technology allows one to fill in the missing pieces of the puzzle that is the sample's fine structure, from the micrometer scale to the nanometer scale, in a way that is impossible with any one technique alone. As we recently outlined when presenting a dedicated journal issue about 'Correlative Microscopy' the development and application of CM has definitely not come to an end just yet (Braet and Geerts 2009). At the present time, we have reached the stage that CM is accepted as a standard, or 'routine', cell-analysis technique, and one in which recent technological advances in molecular and structural biology methods are nicely entwined. With time, we will see more and more research papers appearing that have employed this microscopy technique.

This gives one pause to ask: what we can expect for CM in the foreseeable future? Obviously, CM technology has evolved gradually over the last four decades (Geissinger 1974), with the arsenal of hardware and software tools for CM as well as the number of dedicated CM papers increasing as more researchers have become convinced of its power to dissect cells' architecture over multiple length scales. Currently, the areas to watch out for are 'smart' probes that yield signals at high spatial resolutions and the development of new standardized sample preparation methods for producing accurate, artifact-free, and reproducible CM data. There is also consensus that much can be expected from dedicated cryo-sample preparation (McDonald 2009) and from in situ methods for sample manipulation (Hekking et al. 2009; Mironov and Beznoussenko 2009). Nowadays, several companies offer solutions for rapid transfer of vitrified samples across microscopy platforms or stages that allow precise relocation of the sample between LM and EM platforms. Another interesting development is the way that more and more microscopy platforms are evolving towards 'Integrated Microscopy' (IM). Commercially available solutions are already available for integrated X-ray microtomography (micro-CT) and scanning electron microscopy. Then there is the elegant paper by Agronkaia and colleagues who demonstrated the first fully integrated imaging with fluorescence microscopy and TEM in a single column (Agronskaia et al. 2008) and the recent report on a fully integrated light optical- and scanning electron microscopy platform (Nishiyama et al. 2010). This does not mean, however, that all the efforts in the development of CM tools were a waste of time. On the contrary, optimized methods for sample-relocation, for CM-labeling, and for physical fixation will all be directly applicable to this new way of integrated imaging. And the available CM knowledge will undoubtedly facilitate the implementation of IM technology.

References

Agronskaia AV, Valentijn JA, van Driel LF, Schneijdenberg CT, Humbel BM, van Bergen En Henegouwen PM, Verkleij AJ, Koster AJ, Gerritsen HC (2008) Integrated fluorescence and transmission electron microscopy. J Struct Biol 164:183–189

Albrecht RM, Goodman SL, Simmons SR (1989) Distribution and movement of membrane-associated platelet glycoproteins: use of colloidal gold with correlative video-enhanced light microscopy, low-voltage high-resolution scanning electron microscopy, and high-voltage transmission electron microscopy. Am J Anat 185:149–164

Albrecht RM, Olorundare OE, Simmons SR, Loftus JC, Mosher DF (1992) Use of correlative microscopy with colloidal gold labeling to demonstrate platelet receptor distribution and movement. Methods Enzymol 215:456–479

Biel SS, Kawaschinski K, Wittern KP, Hintze U, Wepf R (2003) From tissue to cellular ultrastructure: closing the gap between micro- and nanostructural imaging. J Microsc 212:91–99

Braet F, Ratinac K (2007) Creating next-generation microscopists: structural and molecular biology at the crossroads. J Cell Mol Med 11:759–763

Braet F, Geerts WJ (2009) Foreword to the themed issue on correlative microscopy. J Microsc 235:239–240

Braet F, Spector I, Shochet NR, Crews P, Higa T, Menu E, De Zanger R, Wisse E (2002) The new anti-actin agent dihydrohalichondramide reveals fenestrae-forming centers in hepatic endothelial cells. BMC Cell Biol 3:7

Braet F, Wisse E, Bomans P, Frederik P, Geerts W, Koster A, Soon L, Ringer S (2007) Contribution of high-resolution correlative imaging techniques in the study of the liver sieve in three-dimensions. Microsc Res Tech 70:230–242

Burton GJ, Thurley KW, Skepper JN (1991) A technique for correlative scanning and transmission electron microscopy of individual human placental villi: an example demonstrating syncytial sprouts in early gestation. Scan Microsc 5:451–458

Capani F, Saraceno E, Boti VR, Aon-Bertolino L, Fernández JC, Gato F, Kruse MS, Giraldez L, Ellisman MH, Coirini H (2008) A tridimensional view of the organization of actin filaments in the

central nervous system by use of fluorescent photooxidation. Biocell 32:1–8

Chang JC, Su HL, Hsu SH (2008) The use of peptide-delivery to protect human adipose-derived adult stem cells from damage caused by the internalization of quantum dots. Biomaterials 29:925–936

Chen I, Ting AY (2005) Site-specific labeling of proteins with small molecules in live cells. Curr Opin Biotechnol 16:35–40

Cheutin T, Sauvage C, Tchélidzé P, O'Donohue MF, Kaplan H, Beorchia A, Ploton D (2007) Visualizing macromolecules with fluoronanogold: from photon microscopy to electron tomography. Methods Cell Biol 79:559–574

Cowieson NP, Kobe B, Martin JL (2008) United we stand: combining structural methods. Curr Opin Struct Biol 18:617–622

Dahan M, Lévi S, Luccardini C, Rostaing P, Riveau B, Triller A (2003) Diffusion dynamics of glycine receptors revealed by single-quantum dot tracking. Science 302:442–445

Darien BJ, Sims PA, Kruseelliott KT, Homan TS, Cashwell RJ, Cooley AJ, Albrecht RM (1995) Use of colloidal gold and neutron-activation in correlative microscopic labeling and label quantitation. Scan Microsc 9:773–780

Deerinck TJ (2008) The application of fluorescent quantum dots to confocal, multiphoton, and electron microscopic imaging. Toxicol Pathol 36:112–116

Deerinck TJ, Martone ME, Lev-Ram V, Green DP, Tsien RY, Spector DL, Huang S, Ellisman MH (1994) Fluorescence photooxidation with eosin: a method for high resolution immunolocalization and in situ hybridization detection for light and electron microscopy. J Cell Biol 126:901–910

Deerinck TJ, Giepmans BNG, Smarr BL, Martone ME, Ellisman MH (2007) Light and electron microscopic localization of multiple proteins using quantum dots. Methods Mol Biol 374:43–53

DeFelipe J, Fairén A (1993) A simple and reliable method for correlative light and electron microscopic studies. J Histochem Cytochem 41:769–772

Derfus AM, Chan WCW, Bhatia SM (2004) Intracellular delivery of quantum dots for live cell labeling and organelle tracking. Adv Mater 16:961–966

Donnell C, Hyde B, Dowling EA (1988) Correlative light and scanning electron-microscopy of endometrium in postmenopausal hormone replacement candidates. Mod Pathol 1:A25–A25

Dubertret B, Skourides P, Norris DJ, Noireaux V, Brivanlou AH, Libchaber A (2002) In vivo imaging of quantum dots encapsulated in phospholipid micelles. Science 298:1759–1762

Ellis EA (2008) Correlative transmission microscopy: cytochemical localization and immunocytochemical localization in studies of oxidative and nitrosative stress. Methods Mol Biol 477:41–48

Fomina AF, Deerinck TJ, Ellisman MH, Cahalan MD (2003) Regulation of membrane trafficking and subcellular organization of endocytic compartments revealed with FM1-43 in resting and activated human T cells. Exp Cell Res 291:150–166

Frey TG, Sun MG (2008) Correlated light and electron microscopy illuminates the role of mitochondrial inner membrane remodeling during apoptosis. Biochim Biophys Acta 1777:847–852

Fucikova A, Valenta J, Pelant I, Brezina V (2009) Novel use of silicon nanocrystals and nanodiamonds in biology. Chem Pap 63:704–708

Geissinger HD (1974) A precise stage arrangement for correlative microscopy for specimens mounted on glass slides, stubs or EM grids. J Microsc 100:113–117

Giepmans BN (2008) Bridging fluorescence microscopy and electron microscopy. Histochem Cell Biol 130:211–217

Giepmans BN, Deerinck TJ, Smarr BL, Jones YZ, Ellisman MH (2005) Correlated light and electron microscopic imaging of multiple endogenous proteins using Quantum dots. Nat Methods 10:743–749

Goodman SL, Albrecht RM (1987) Correlative light and electron-microscopy of platelet-adhesion and fibrinogen receptor expression using colloidal-gold labeling. Scan Microsc 1:727–734

Grabenbauer M, Geerts WJ, Fernadez-Rodriguez J, Hoenger A, Koster AJ, Nilsson T (2005) Correlative microscopy and electron tomography of GFP through photooxidation. Nat Methods 14:857–862

Hainfeld JF, Furuya FR (1992) A 1.4-nm gold cluster covalently attached to antibodies improves immunolabeling. J Histochem Cytochem 40:177–184

Hekking LH, Lebbink MN, De Winter DA, Schneijdenberg CT, Brand CM, Humbel BM, Verkleij AJ, Post JA (2009) Focused ion beam-scanning electron microscope: exploring large volumes of atherosclerotic tissue. J Microsc 235:336–347

Hirabayashi Y, Yamada K (1998) A histochemical approach to correlative light and electron microscopic detection of acidic glycoconjugates by a sensitized high iron diamine method. J Histochem Cytochem 46:767–770

Ho Y-P, Leong KW (2010) Quantum dot-based theranostics. Nanoscale 2:60–68

Hwang RD, Chen CC, Knecht DA (2009) ReAsH: another viable option for in vivo protein labelling in Dictyostelium. J Microsc 234:9–15

Jahn KA, Braet F (2008) Monitoring membrane rafts in colorectal cancer cells by means of correlative fluorescence electron microscopy (CFEM). Micron 39:1393–1397

Jahn K, Barton D, Braet F (2007) Correlative fluorescence- and scanning, transmission electron microscopy for biomolecular investigation. In: Díaz J, Méndez-Vilas A (eds) Modern research and educational topics in microscopy. Formatex Press, Badajoz, pp 203–211

Jahn KA, Barton DA, Su Y, Riches J, Kable EPW, Soon LL, Braet F (2009) Correlative fluorescence and transmission electron microscopy imaging of the actin cytoskeleton of whole-mount (breast) cancer cells. J Microsc 235:282–292

Kushida T, Nagato Y, Iijima H, Kushida H (1993) Correlative light and electron microscopy of the same sections embedded in HPMA, Quetol 523 and MMA. Okajimas Folia Anat Jpn 69:277–287

Larson DR, Zipfel WR, Williams RM, Clark SW, Bruchez MP, Wise FW, Webb WW (2003) Water-soluble quantum dots for multiphoton fluorescence imaging in vivo. Science 300:1434–1436

Lin MZ, Wang L (2008) Selective labeling of proteins with chemical probes in living cells. Physiology 23:131–141

Lübke J (1993) Photoconversion of diaminobenzidine with different fluorescent neuronal markers into a light and electron microscopic dense reaction product. Microsc Res Tech 24:2–14

Martin BR, Giepmans BN, Adams SR, Tsien RY (2005) Mammalian cell-based optimization of the biarsenical binding tetracycteine motif for improved fluorescence and affinity. Nat Biotechnol 23:1308–1314

Mattheakis LC, Dias JM, Choi Y-J, Gong J (2004) Optical coding of mammalian cells using semiconductor quantum dots. Anal Biochem 327:200–208

McCann CM, Bareyre FM, Lichtman JW, Sanes JR (2005) Peptide tags for labeling membrane proteins in live cells with multiple fluorophores. Biotechniques 38:945–952

McDonald K (2009) A review of high-pressure freezing preparation techniques for correlative light and electron microscopy of the same cells and tissues. J Microsc 235:273–281

McDonald LW, Hayes TL (1969) Correlation of scanning electron microscope and light microscope images of individual cells in human blood and blood clots. Exp Mol Pathol 10:186–198

Meißlitzer-Ruppitsch C, Röhrl CR, Neumuller J, Pavelka M, Ellinger A (2009) Photooxidation technology for correlated light and electron microscopy. J Microsc 235:322–335

Miller SE, Howell DN (1997) Concerted use of immunologic and ultrastructural analyses in diagnostic medicine: Immunoelectron microscopy and correlative microscopy. Immunol Invest 26:29–38

135

Mironov AA, Beznoussenko GV (2009) Correlative microscopy: a potent tool for the study of rare or unique cellular and tissue events. J Microsc 235:308–321

Mironov AA, Polishchuk RS, Luini A (2000) Visualizing membrane traffic in vivo by combined video fluorescence and 3D electron microscopy. Trends Cell Biol 8:349–353

Monosov EZ, Wenzel TJ, Lüers GH, Heyman JA, Subramani S (1996) Labeling of peroxisomes with green fluorescent protein in living P. pastoris cells. J Histochem Cytochem 44:581–589

Morphew MHW, Bjorkman PJ, McIntosh JR (2008) Silver enhancement of nanogold particles during freeze substitution for electron microscopy. J Microsc 230:263–267

Nishiyama H, Suga M, Ogura T, Maruyama Y, Koizumi M, Mio K, Kitamura S, Sato C (2010) Atmospheric scanning electron microscope observes cells and tissues in open medium through silicon nitride film. J Struct Biol 169:438–449

Nisman R, Dellaire G, Ren Y, Li R, Bazett-Jones DP (2004) Application of quantum dots as probes for correlative fluorescence, conventional, and energy-filtered transmission electron microscopy. J Histochem Cytochem 52:13–18

Nixon SJ, Webb RI, Floetenmeyer M, Schieber N, Lo HP, Parton RG (2009) A single method for cryofixation and correlative light, electron microscopy and tomography of zebrafish embryos. Traffic 10:131–136

Nykänen M (2009) Correlation of light with electron microscopy: a correlative microscopy platform. In: Goldys EM (ed) Fluorescence applications in biotechnology and life sciences. Wiley-Blackwell, Hoboken, pp 141–156

Oehring H, Halbhuber KJ (1991) Employment of merocyanine 540 fluorescence to form diaminobenzidine (DAB) oxidation product: a photoconversion method for the visualization of erythrocyte membrane fluidity for light and electron microscopy. Acta Histochem 90:127–134

Pagano RE, Sepanski MA, Martin OC (1989) Molecular trapping of a fluorescent ceramide analogue at the Golgi apparatus of fixed cells: interaction with endogenous lipids provides a trans-Golgi marker for both light and electron microscopy. J Cell Biol 109:2067–2079

Park H, Hanson GT, Duff SR, Selvin PR (2004) Nanometre localization of single ReAsH molecules. J Microsc 216:199–205

Peachey LD, Ishikawa H, Murakami T (1996) Correlated confocal and intermediate voltage electron microscopy imaging of the same cells using sequential fluorescence labeling, fixation, and critical point dehydration. Scan Microsc 10:237–247

Peng XG (2003) Mechanisms for the shape-control and shape-evolution of colloidal semiconductor nanocrystals. Adv Mater 15:459–463

Perinetti G, Müller T, Spaar A, Polishchuk R, Luini A, Egner A (2009) Correlation of 4Pi and electron microscopy to study transport through single Golgi stacks in living cells with super resolution. Traffic 10:379–391

Plitzko JM, Rigort A, Leis A (2009) Correlative cryo-light microscopy and cryo-electron tomography: from cellular territories to molecular landscapes. Curr Opin Biotechnol 20:83–89

Powell RD, Halsey CM, Hainfeld JF (1998) Combined fluorescent and gold immunoprobes: reagents and methods for correlative light and electron microscopy. Microsc Res Tech 42:2–12

Rash JE, Yasumura T, Dudek FE (1998) Ultrastructure, histological distribution, and freeze-fracture immunocytochemistry of gap junctions in rat brain and spinal cord. Cell Biol Int 22:731–749

Razi M, Tooze SA (2009) Correlative light and electron microscopy. Methods Enzymol 452:261–275

Reynolds AM, Sculimbrene BR, Imperiali B (2008) Lanthanide-binding tags with unnatural amino acids: sensitizing Tb3+ and Eu3+ luminescence at longer wavelengths. Bioconjug Chem 19:588–591

Rieder CL, Bowser SS (1985) Correlative immunofluorescence and electron-microscopy on the same section of epon-embedded material. J Histochem Cytochem 33:165–171

Robinson JM, Vandré DD (1997) Efficient immunocytochemical labeling of leukocyte microtubules with FluoroNanogold: an important tool for correlative microscopy. J Histochem Cytochem 45:631–642

Säälik P, Padari K, Niinep A, Lorents A, Hansen M, Jokitalo E, Langel Ü, Pooga M (2009) Protein delivery with transportans is mediated by caveolae rather than flotillin-dependent pathways. Bioconjug Chem 20:877–887

Schmued LC, Snavely LF (1993) Photoconversion and electron microscopic localization of the fluorescent axon tracer fluoro-ruby (rhodamine-dextran-amine). J Histochem Cytochem 41:777–782

Shaner NC, Steinbach PA, Tsien RY (2005) A guide to choosing fluorescent proteins. Nat Methods 2:905–909

Simmons SR, Pawley JB, Albrecht RM (1990) Optimizing parameters for correlative immunogold localization by video-enhanced light microscopy, high-voltage transmission electron microscopy, and field emission scanning electron microscopy. J Histochem Cytochem 38:1781–1785

Sletten EM, Bertozzi CR (2009) Bioorthogonal chemistry: fishing for selectivity in a sea of functionality. Angew Chem Int Ed Eng 48:6974–6998

Smith A, Ruan G, Rhyner M, Nie S (2006) Engineering luminescent quantum dots for in vivo molecular and cellular imaging. Ann Biomed Eng 34:3–14

Sosinsky GE, Giepmans BN, Deerinck TJ, Gaietta GM, Ellisman MH (2007) Markers for correlated light and electron microscopy. Methods Cell Biol 79:575–591

Subramaniam S (2005) Bridging the imaging gap: visualizing subcellular architecture with electron tomography. Curr Opin Microbiol 8:316–322

Sun MG, Williams J, Munoz-Pinedo C, Perkins GA, Brown JM, Ellisman MH, Green DR, Frey TG (2007) Correlated three-dimensional light and electron microscopy reveals transformation of mitochondria during apoptosis. Nat Cell Biol 9:1057–1072

Sunbul M, Yen M, Zou Y, Yin J (2008) Enzyme catalyzed site-specific protein labeling and cell imaging with quantum dots. Chem Commun 45:5927–5929

Swanson JA, Peters PJ (2005) Subcellular imaging technologies - microscopic visual thinking. Curr Opin Microbiol 8:313–315

Takizawa T, Robinson JM (2000) Analysis of antiphotobleaching reagents for use with fluoronanogold in correlative microscopy. J Histochem Cytochem 48:433–436

Verkade P (2008) Moving EM: the Rapid Transfer System as a new tool for correlative light and electron microscopy and high throughput for high-pressure freezing. J Microsc 230:317–328

Walling MA, Novak JA, Shepard JR (2009) Quantum dots for live cell and in vivo imaging. Int J Mol Sci 10:441–491

Walther C, Meyer K, Rennert R, Neundorf I (2008) Quantum dot-carrier peptide conjugates suitable for imaging and delivery applications. Bioconjug Chem 19:2346–2356

Wynford-Thomas D, Jasani B, Newman GR (1986) Immunohistochemical localization of cell surface receptors using a novel method permitting simple, rapid and reliable LM/EM correlation. Histochem J 18:387–396

Zhang Y, So MK, Rao J (2006) Protease-modulated cellular uptake of quantum dots. Nano Lett 6:1988–1992

Zipfel W, Williams R, Webb W (2003) Nonlinear magic: multiphoton microscopy in the biosciences. Nat Biotechnol 21:1369–1377